Tailoring Coulomb correlations in twisted WSe_2 bilayers

Philipp Merkl[1], Fabian Mooshammer[1], Samuel Brem[2], Anna Girnghuber[1], Kai-Qiang Lin[1], Leonard Weigl[1], Chaw-Keong Yong[1], Roland Gillen[3], Janina Maultsch[3], John M. Lupton[1], Ermin Malic[2] and Rupert Huber[1]

[1]*Department of Physics, University of Regensburg, 93040 Regensburg, Germany*
[2]*Department of Physics, Chalmers University of Technology, Gothenburg, Sweden*
[3] *Institute of Condensed Matter Physics, Friedrich-Alexander University Erlangen-Nürnberg, Germany*
philipp1.merkl@ur.de

Abstract: Phase-locked few-cycle mid-infrared pulses trace how the twist angle alone renormalizes the binding energy of excitons in twisted WSe_2 homobilayers by a factor of two and tunes their lifetime by a factor of twenty.

Solid-state physics is the science of many-body interactions. To tackle the formidable many-body problem of typically 10^{23} charged particles per cm^3 of a solid, Lev Landau introduced the concept of quasiparticles. These fictitious entities describe particles dressed by their many-body interactions and define key properties of a solid. Usually, the internal structure and the mutual interaction of quasiparticles are material specifics, but van der Waals layered materials provide a new tuning knob: the twist angle between adjacent layers can turn the semimetal graphene into a Mott insulator [1], superconductor [2], or ferromagnet [3]. Topological phases [4] and shear solitons [5] have been discussed for twisted bilayers of transition-metal dichalcogenides. Twist-induced changes of the single-particle band structure have manifested in excitonic interband resonances [6], but a precise understanding of the underlying Coulomb correlations has remained challenging, even though it is key to tailoring novel functionalities of matter.

Here, we isolate how the internal structure and mutual interaction of excitons in WSe_2 BLs can be tailored by the twist angle alone [7]. To this end, we resonantly inject 1*s* A excitons in BLs with variable twist angles using 100-fs near-infrared (NIR) laser pulses (Fig. 1a, yellow intensity envelope). After a variable pump-probe delay time t_{pp}, phase-locked MIR pulses (Fig. 1a, orange wave) interrogate Lyman-like 1*s*−2*p* transitions of all optically bright and dark excitons (Fig. 1b, orange arrows). By monitoring the characteristic changes of the MIR waveform after transmission through the photo-excited BL using electro-optic sampling, we extract the complex-valued dielectric response of the non-equilibrium system [8]. Therein, the excitonic 1*s*−2*p* transition manifests as a characteristic resonance (Fig. 1c,d). It is noteworthy that by tracing the absorption at the 1*s*-2*p* resonance, we monitor all excitons, irrespective of interlayer optical selection rules. This is in sharp contrast to optical interband probes, such as photoluminescence studies, which are sensitive to optically bright species only. Remarkably, the 1*s*–2*p* transition en-

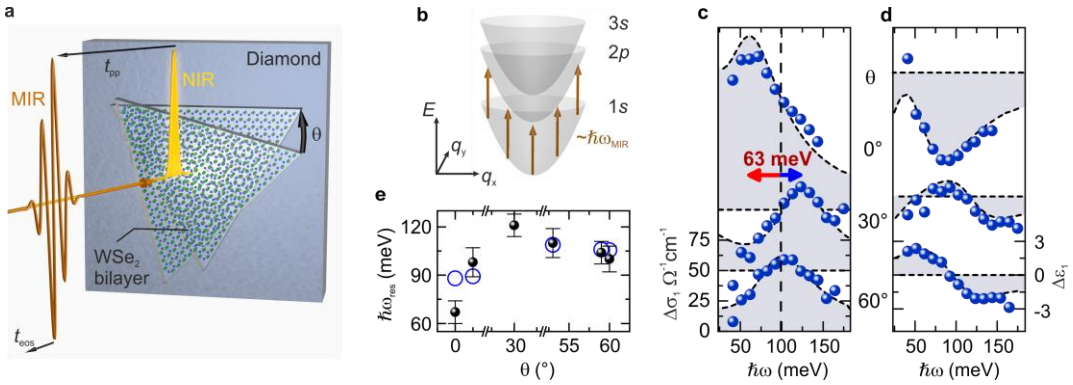

Fig. 1: Twist-tailoring excitons. **a**, Sketch of the experiment, where a near-infrared (NIR) pump pulse (yellow intensity envelope) optically injects 1*s* A excitons in the WSe_2 BLs. The excited sample is probed by a MIR waveform (orange curve). **b**, Exciton dispersion for a given orbital quantum number depicted as a function of the center-of-mass momentum q (grey paraboloids). Red arrows indicate the 1*s*–2*p* transitions corresponding to the energy $\hbar\omega_{MIR}$. **c**, **d**, Pump-induced changes of the real parts of the optical conductivity $\Delta\sigma_1$ (**c**) and the dielectric function $\Delta\varepsilon_1$ (**d**) for a fixed pump-probe delay time t_{pp} = 5.1 ps as a function of the photon energy for samples with different twist angles θ. Blue spheres: experimental data (pump fluence Φ = 27 μJ/cm²; sample temperature, 5 K). Grey shaded areas: phenomenological model. The dashed line and the blue/red arrow indicate the blue/red shift of the 1*s*–2*p* resonance energy $\hbar\omega_{res}$. **e**, $\hbar\omega_{res}$ (black spheres) extracted from the data in **c**, **d** and derived from the microscopic theory (blue circles) as function of θ. For θ = 30°, microscopic calculations of hybrid excitons were not feasible.

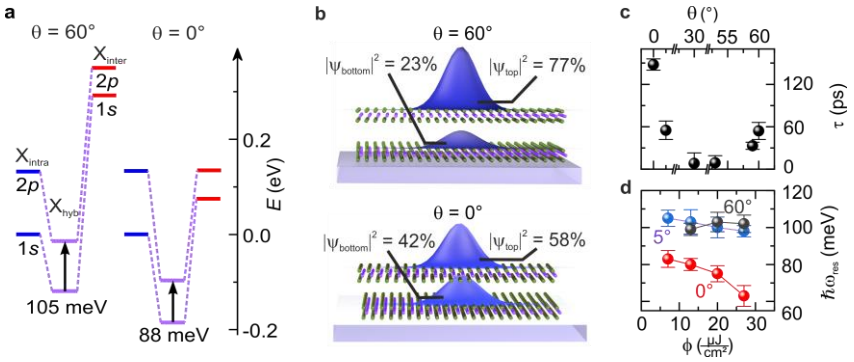

Fig. 2: **a**, Hybridization of 1*s* and 2*p* excitons X_{hyb} lowers the energy levels (magenta lines) with respect to X_{intra} and X_{inter} (blue/red lines). The situation is sketched for θ = 60°and 0°. Zero energy is set to 1*s* X_{intra} at θ = 60°. The vertical black arrows mark respective 1*s*–2*p* transition energies. **b**, Calculated probability density of the electron within the two layers for X_{hyb} for θ = 60°, 50°, and 0°, where the hole is chosen to remain at a fixed position in the top layer. **c**, Exciton decay time τ as a function of θ. **d**, $\hbar\omega_{res}$ for different pump fluences Φ at t_{pp} = 5.1 ps for different θ.

ergy – a direct measure for the exciton binding energy is renormalized by as much as a factor of two by varying the twist angle (Fig. 1e, black spheres). These findings are explained by a fully quantum mechanical model, which allows us to identify the underlying microscopic origin: hybridization between different excitonic species in the photo-excited BL. In WSe_2 BLs, K-Λ excitons represent the energetic ground state. Here, electron and hole can reside in the same or the adjacent layer, forming intra- (X_{intra}) or interlayer excitons (X_{inter}), respectively. Strong electron interlayer hopping [9] in the Λ valley then gives rise to hybrid excitons (X_{hyb}) (see Fig. 2a). Their properties critically depend on the twist angle as it determines the wavefunction overlap of X_{intra} and X_{inter} in momentum space. Furthermore, the exact reduction in energy upon hybridization strongly depends on the orbital quantum number of the individual excitonic levels. Thus, the 1*s*–2*p* resonance is renormalized by a variable amount as a function of twist angle, in excellent agreement with the experiment (Fig. 1e, blue circles). The highest degree of hybridization is observed for θ = 0°, where the initial energy levels are almost perfectly degenerate since both states contain electrons from the same valley and are therefore not offset by spin-orbit splitting. Hence, an even smaller 1*s*–2*p* transition energy is observed as compared to the pristine bilayer (θ = 60°).

The variable degree of interlayer hybridization of excitons also allows us to tune the exciton lifetime (Fig 2c). By changing the twist angle, the orbital overlap of the conduction band states shrinks, which impedes interlayer hopping, thus effectively decoupling the layers. With both electron and hole wavefunctions overlapping strongly in the same layer, the recombination lifetime of the exciton drops, reaching a minimum at θ = 30°. In contrast, the electron is delocalized strongly over both layers for θ = 0° (Fig. 2b), which distinctly extends the exciton lifetime. Furthermore, the twist-angle controlled interlayer delocalization can also be employed to tune the interaction among excitons for θ = 0° (Fig. 2d). Microscopically, strongly delocalized excitons mutually screen the Coulomb interaction more effectively reducing the binding energy with increasing exciton density.

In conclusion, we reveal systematic changes of the binding energy, lifetime and exciton-exciton interaction of excitons in WSe_2 BLs depending on twist angle, which are quantitatively reproduced by a microscopic model describing the underlying hybridization effects. These findings underpin a qualitatively new way of fine-tuning the internal structure of excitons in TMDs and controlling the electronic and optical properties in van der Waals homobilayers. Tailoring many-body correlations over a large energy range can now be systematically extended to the full library of two-dimensional crystals, which should guide the search for novel electronic phases in van der Waals heterostructures.

[1] Cao, Y. *et al.* "Correlated insulator behaviour at half-filling in magic-angle graphene superlattices", *Nature* **556**, 80–84 (2018).
[2] Cao, Y. *et al.* "Unconventional superconductivity in magic-angle graphene superlattices", *Nature* **556**, 43–50 (2018).
[3] Sharpe, A. L. *et al.* "Emergent ferromagnetism near three-quarters filling in twisted bilayer graphene", *Science* **365**, 605–608 (2019).
[4] Wu, F., Lovorn, T. & MacDonald, A. H. "Topological Exciton Bands in Moiré Heterojunctions", *Phys. Rev. Lett.* **118**, 147401 (2017).
[5] Naik, M. H. & Jain, M. "Ultraflatbands and Shear Solitons in Moiré Patterns of Twisted Bilayer Transition Metal Dichalcogenides", *Phys. Rev. Lett.* **121**, 266401 (2018).
[6] Alexeev, E. M. et al. "Resonantly hybridized excitons in moiré superlattices in van der Waals heterostructures", *Nature* **567**, 81–86 (2019).
[7] Merkl, P. et al. "Twist-tailoring Coulomb correlations in van der Waals homobilayers", *Nat. Commun.* **11**, 2167 (2020).
[8] Merkl, P. et al. "Ultrafast transition between exciton phases in van der Waals heterostructures", Nat. Mater. 18, 691–696 (2019).
[9] Liu, G.-B., Xiao, D., Yao, Y., Xu, X. & Yao, W. "Electronic structures and theoretical modelling of two-dimensional group-VIB transition metal dichalcogenides", *Chem. Soc. Rev.* **44**, 2643–2663 (2015).